



Coordinated Electric Vehicle Charging Strategy in Microgrids Containing PV System

Nuh ERDOĞAN^{1,2*}, Fatih ERDEN², Tuncay ALTUN¹

¹Department of Electrical Engineering, University of Texas at Arlington, United States.

²Electrical and Electronics Engineering, Atılım University, Turkey.

Article Info

Received: 25/12/2016

Accepted: 08/03/2017

Keywords

Coordinated charging
Microgrid
Photovoltaic (PV)
Plug-in electric vehicle
(PEV)

Abstract

This study investigates the impact of different plug-in electric vehicles (PEVs) charging strategies in grid-connected microgrid containing PV generation system. Two different coordinated charging strategies with constant and variable power rates are proposed to increase the utilization of PV energy in the microgrid and decrease the undesired peaks due to PEV charging loads on the grid. First, based on forecasted base load and PV generation data, a microgrid central controller (MGCC) performs an offline operation to determine a charging zone. Then, in real time operation, it updates the charging zone and determines the charging profiles for each PEV by considering the base load and PV generation data instantly. The performance of the proposed strategy is assessed through a part of Cornell University microgrid with real data, and compared with other charging methods in terms of PV system energy usage percentage, energy supplied and peak demand from the grid by presenting numerical results. The results show that the proposed charging strategy can achieve increased PV utilization and reduced peak demand from the grid substantially.

1. INTRODUCTION

Ever increasing environmental concerns, reducing fuel reserves, and efforts to reduce carbon emissions have led to distributed renewable energy resources (DRES) to become widespread in the last decade [1]. These energy sources are usually established in residential and industrial areas forming microgrids which can be operated both in grid connected and islanded modes. More recently, energy security and reliability concerns have increased the interest in microgrids due to potential vulnerability of the large and centralized power system [2]. As flexible elements of future smart grids, microgrids have been considered to lead the way for improving the power system resiliency [2], [3]. However, ensuring reliability and resiliency requirements in distribution systems with microgrids becomes more challenging due to ever increasing the number of DRES and PEVs in the microgrids [4].

In the composition of future smart grids, the interaction of microgrids and PEVs is likely to increase in coming decades given the expected penetration of DRES and PEVs [5]. Uncontrolled adaptation of PEVs into microgrids with a high rate may result in undesirable effects such as frequency and voltage deviations [6]. Simply, shifting PEV charging time without charging strategy to the time when renewable energy is abundant, causes a non-uniform load profile with undesired peak loads due to charging many PEVs simultaneously [7]. Thus, coordinated charging becomes indispensable for large-scale penetration of PEVs into microgrids. Coordinated charging manages PEV charging loads effectively to mitigate the undesirable impacts on the grid [8]. It enables a charging flexibility that can be used to integrate higher share of intermittent renewable energy sources into the grid [9]-[11], to minimize the cost of microgrid operation [12] and to provide services, e.g., peak shaving [8], voltage and frequency regulation [6], [13]. Therefore, coordinated DRES - PEVs energy dispatching has been one of the main foci for many researchers in recent years [10]-[19].

The research studies on microgrids being in interaction with PEVs can be roughly classified into two groups. The first group [3], [4], [12], [13] exploit PEVs to maintain the stability in islanded microgrids. In these studies, PEVs are used for voltage and frequency regulation control by taking advantage of their

*Corresponding author, e-mail: nuh.erdogan@uta.edu

charging flexibility and storage capability. Gouveia et al in [3], [4] proposes a droop-based controller for frequency regulation in an islanded microgrid. The decisions for charging/discharging PEVs are made by a microgrid central controller (MGCC) according to a frequency-droop characteristic. However, these studies do not consider PEVs mobility. In [12] and [13], multi-stage centralized controller is proposed to avoid the inaccuracies stemming from forecasted renewable energy generation and PEV mobility characteristics.

The second group [10], [11], [14]-[19] focus on energy dispatching in grid connected microgrids with intermittent renewable resources (e.g., wind/solar power etc.) and PEVs. The aim is to improve the utilization of renewable energy resources within the microgrid, and to reduce the impact of the charging demand on the grid while ensuring the PEVs charging powers. In [16], a real-time power allocation algorithm for PEVs in commercial microgrids with PVs is proposed. In this study, the desired state-of-charge (SOC) level of battery at departure time is not always guaranteed, which is inconvenient from the PEV user perspective. The studies in [11], [14], [17]–[19] address very unrealistic scenarios by assuming deterministic PEV mobility and perfect renewable energy forecasting. In [11], for power matching between wind energy and the demand, PEVs are considered to be charged/discharged at any time without taking into account the PEVs' mobility and their SOC levels. In [17] only PEV loads are considered in grid-connected microgrid. Also, PEVs' mobility characteristics, i.e., SOC levels, and plug-in and plug-off times, are not included in [14] and [18]. As a conclusion, the integration of PEVs in microgrid setting with stochastic PEV mobility characteristics has not been explored sufficiently. Additionally, an accurate tracking the renewable power generation profile is needed for maximizing the utilization of renewable energy sources as well as meeting the dynamic power demands in microgrids.

This study investigates PEV charging algorithms to increase the utilization of PV energy in a microgrid and to decrease the undesired impact of charging loads on the grid. For this purpose, a coordinated PEV charging strategy is developed for a grid connected microgrid containing PV system. The proposed strategy makes the charging profiles track the PV generation profile by taking into account PEVs' stochastic mobility characteristics. Thus, the utilization of PV system energy is increased, and the energy supplied as well as the peak demand from the grid is reduced. From the PEV user perspectives, the desired SOC level, i.e. full charging, is provided at departure time. The proposed algorithm is tested on real PV generation and load profile data. The performance of the strategy is quantified and compared with other charging methods in terms of PV system energy usage percentage, energy supplied and peak demand from the grid by presenting numerical results.

2. PV-PEV MICROGRID SYSTEM MODELING

2.1. System Description of Typical Microgrid

The structure diagram of the microgrid used in this study is depicted in Fig.1. This typical grid-connected microgrid can be described as a system that has PV generation arrays with a dc/ac inverter, loads, including PEVs and their charging station and a MGCC. The PV generation system is connected to point of common coupling (PCC) through the dc/ac inverter that is controlled by the MGCC with a wireless/wired communication set-up. The charging station consists of electric vehicle supply equipments (EVSEs) having unidirectional ac/dc converter that communicates with the MGCC through the communication link.

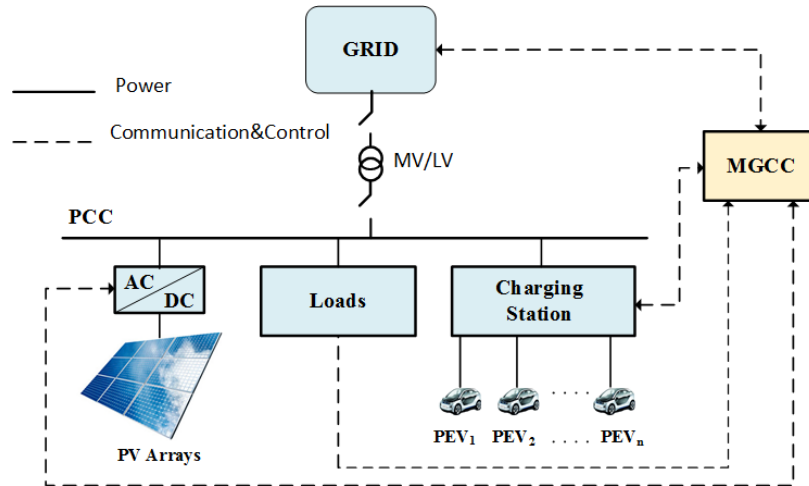


Figure 1. Typical representation of the examined microgrid.

As a decision maker, MGCC is the vital component of a microgrid. MGCC manages and controls the microgrid based on the embedded algorithm and information obtained from main grid, dc/ac inverter connected to PV arrays, and charging station coupled with the PEVs. MGCC might have several duties namely proper coordination of power generation and load demand, satisfactory control of microgrid either in grid connected or islanded mode, microgrid protection and providing stability in case fault occurrences [3]. In this study, the additional objective of MGCC is to adjust the PEVs charging loads dynamically in order to track the PV generation profile. Using the communication link, the MGCC receives PV generation and base load profiles instantly, as well as the PEV mobility characteristics from the EVSEs. The MGCC determines the charging power profile for each PEV with the coordinated charging algorithm developed in Section 3 so as to create a total charging power to track the PV generation profile. The MGCC dynamically updates the charging power references in accordance with the PV generation and microgrid load profile characteristics at each time step.

2.2. System Modeling

The aggregated load (kW) refers the total load demand in the examined microgrid, which is defined as,

$$p_{aggr}(t) = p_{base}(t) + \sum_{i=1}^n p_{ch,i}(t), \tag{1}$$

where, $p_{base}(t)$ and $p_{ch,i}(t)$ are base and charging load of the i^{th} PEV at time t respectively, and n is the number of PEVs. The total power supplied in the microgrid must satisfy the total load demand. Thus, the power supplied from the grid can be found as,

$$p_{supply}(t) = \begin{cases} p_{aggr}(t) - p_{PV}(t) & \text{if } p_{aggr}(t) > p_{PV}(t) \\ 0 & \text{if } p_{aggr}(t) \leq p_{PV}(t) \end{cases} \tag{2}$$

where, $p_{PV}(t)$ is the power (kW) generated by the PV system at time t .

3. PEV CHARGING STRATEGIES

Existing PEV charger hardware and technologies allow charging at either variable or constant (rated) powers [20]. Using these power profiles, charging process can be performed in uncoordinated and coordinated manners [21]. Uncoordinated charging refers the charging at charger power rating while in coordinated charging, PEVs' chargings are managed with centralized and decentralized approaches for better utilization of the power generation assets [22]. Coordinated charging can be performed with two manners. The first approach includes shifting charging loads to off-peak hours where the demand load and the electricity price is lower. In this approach, PEVs are charged at rated power. However, smart charging

strategies are applied in the second approach to adjust dynamically PEV charging profiles based on certain parameters such as the grid load profile, the characteristics of PEVs connected to the grid etc.

3.1. Uncoordinated Charging

To determine the charging power for the i^{th} PEV in Eq. (1), first the energy (kWh) required to fully charge the i^{th} PEV is calculated:

$$E_{ch,i} = (1 - SOC_{initial,i}) \times \frac{C_{B,i}}{\eta}, \quad (3)$$

where, $SOC_{initial,i}$ is the SOC level of that PEV at arrival time, $C_{B,i}$ and η are the nominal battery capacity (kWh) and the on-board charger efficiency of the i^{th} PEV, respectively. Using Eq. (3), the total charging time ($T_{ch,i}$) for the i^{th} PEV to be fully charged at rated charging power can be calculated as,

$$T_{ch,i} = \frac{E_{ch,i}}{P_i^{rated} \times \eta}, \quad (4)$$

where, P_i^{rated} is the rated charging power (kW) of i^{th} PEV. Each of the on-board chargers used in this study are assumed to have a constant 90% operating efficiency and unit power factor at all operating points. Then, the charging power (kW) for the i^{th} PEV can be calculated by Eq. (5).

$$p_{ch,i}(t) = \begin{cases} P_i^{rated}, & \forall t \in [t_{arr,i}, t_{arr,i} + T_{ch,i}] \\ 0, & otherwise \end{cases}, \quad (5)$$

where, $t_{arr,i}$ is the arrival time of the i^{th} PEV vehicle.

As seen from Eq. (5), the charging process is performed at on-board charger power rating without any control fashion. However, in the coordinated charging strategy, PEVs are charged with a time-varying charging power profile which is developed in the next subsection.

3.2. Shifted Charging

In this study, shifted charging are done with uncontrolled and controlled strategies as follow:

3.2.1. Shifted charging with uncontrolled strategy

In this strategy, PEV charging process are first shifted by the MGCC to the time when PV output power is greater than the base load. PEVs are then charged at their charger rating power.

$$p_{ch,i}(t) = \begin{cases} P_i^{rated}, & \forall t \in [t_1, t_1 + T_{ch,i}] \\ 0, & otherwise \end{cases}, \quad (6)$$

where, t_1 refers the first time when PV output and base load profiles intersect, which can be determined as Eq. (10).

3.2.2. Shifted charging with controlled strategy

In this proposed strategy, the initial time to start charging for each PEV is determined in such a way that PEVs are charged fully at the second time of intersection between PV output and base load profiles. In case the departure time for any PEV is less than the second time of intersection, the charging starting time is determined as the PEV is fully charged at departure. This strategy can be modelled as follow:

$$p_{ch,i}(t) = \begin{cases} P_i^{rated}, & \forall t \in [t_2 - T_{ch,i}, t_2], \text{ if } t_2 \leq t_{dept,i} \\ P_i^{rated}, & \forall t \in [t_{dept,i} - T_{ch,i}, t_{dept,i}], \text{ if } t_{dept,i} < t_2 \end{cases}, \quad (7)$$

where, t_2 is the second time of intersection between PV output and base load profiles, which can be determined as Eq. (10). $t_{dept,i}$ is the departure time for i^{th} PEV.

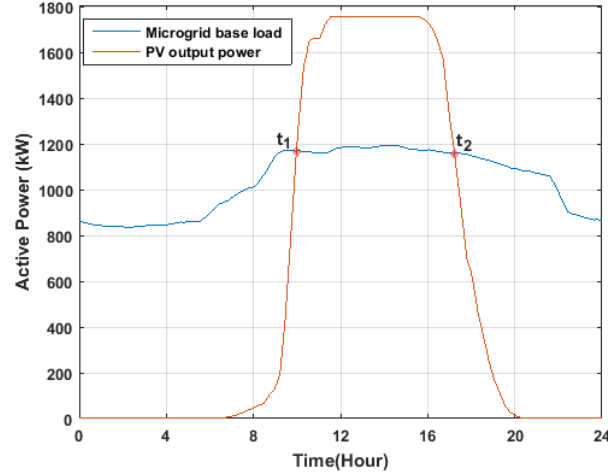


Figure 2. Determination of intersections between base load and PV generation profiles based on forecasted data.

3.3. Development of Coordinated PEV Charging Strategy

Based on all the features and capabilities of the system mentioned above, the proposed coordinated charging strategy is generated to both maximize the utilization of renewable energy in microgrid and minimize the demand power from the grid. The coordinated charging strategy can be casted as mixed integer linear optimization problem, which has objective function, equality and inequality constraints to meet physical requirements. The objective function directly imposes minimization of the demand power; however, maximization of renewable energy utilization is realized by constraints indirectly. This objective function can be formally expressed as follow,

$$\min \left[p_{base}(t) + \sum_{i=1}^n p_{ch,i}(t) - p_{PV}(t) \right] \tag{8}$$

$$\text{subject to} \left[\begin{array}{l} 0 < P_{ch,i}(t) \leq P_i^{rated} \quad \forall t \in [t_{start,i}, t_{finish,i}] \tag{9.a} \\ t_{start,i} - t_{finish,i} = T_i \tag{9.b} \\ t_{arr,i} \leq t_{start,i} \leq t_{dept,i} - T_i \tag{9.c} \\ t_{dept,i} - t_{arr,i} - T_i \geq 0 \tag{9.d} \\ t_1 \leq t_{start,i} \tag{9.e} \\ t_2 \geq t_{finish,i} \tag{9.f} \end{array} \right], \quad i=1,2,\dots,n$$

Eq. (8) always seeks optimal demand power value at each time step, whereas the requirements of Eq. (9) must be provided simultaneously. Eq. (9) stands for the constraints of the linear optimization problem, where, $t_{start,i}$, and $t_{finish,i}$, denote to the charging start and stop times, respectively. $t_{arr,i}$ and $t_{dept,i}$, the arrival and departure times for the i^{th} PEV, respectively. T_i , is the required charging time interval, for i^{th} PEV. t_1 and t_2 are defined in Eq. (10), which is explained in following. The constraints in (9.e) and (9.f) ensure to maximum utilization of PV generation, whereas the constraint in (9.c) guarantees the required SOC level by the departure time, i.e. full charging.(9.a) constraint indicates variable charging power rate in contrast to other charging strategies; with previously explained last three constraints render charging strategy to optimal that implies minimized demand power and maximized renewable energy utilization.(9.b) states the charging period has to be equal to the required charging interval, and (9.d) constraint states that the time PEV is connected to the grid should be equal to or greater than the required charging interval.

As given in Eq.(2), the coordinated charging strategy is trying to meet aggregated load profile as long as PV generation profile is greater than or equal to aggregated load profile. Otherwise PV generation is completely used first and the rest of the aggregated load is absorbed from grid. In the coordinated charging, PEVs are charged during the time interval where the PV generation is greater than the base load, and such that the PEV charging power profiles track the difference between the PV output and base load. For this purpose, the valley power (kW), $p_{valley}(t)$ is first calculated as follow,

$$p_{valley}(t) = \begin{cases} \hat{p}_{PV}(t) - \hat{p}_{base}(t), & \forall t \in [t_1, t_2] \\ 0, & otherwise \end{cases}, \quad (10)$$

where, $\hat{p}_{PV}(t)$ and $\hat{p}_{base}(t)$ are the forecasted PV output power and base load respectively at time t . t_1 is the first time when $\hat{p}_{PV}(t)$ and $\hat{p}_{base}(t)$ intersect, and t_2 is the second time of intersection (Fig. 2). The determination of the base load and PV generation profile is a subject of load/PV generation forecasting and is not investigated in this study. Interest readers are referred to relevant literature [23] and [24]. The MGCC performs an offline operation for this calculation using historical base load and PV generation data which are shown in Fig.2. Then, in real time operation, it updates the charging zone by considering the base load and PV generation data instantly.

Having determined the valley power, the energy of the valley (kWh) for the i^{th} PEV, $E_{valley,i}$, is computed as follows,

$$E_{valley,i} = \int_{t_{start,i}}^{t_{finish,i}} p_{valley}(t) dt, \quad (11)$$

Finally charging power (kW) for the i^{th} vehicle at time t is determined as follows,

$$p_{ch,i}(t) = \begin{cases} \alpha \cdot p_{valley}(t), & \forall t \in [t_{start,i}, t_{finish,i}] \\ 0, & otherwise \end{cases}, \quad (12)$$

where, α is the tracking factor and expressed as

$$\alpha = \frac{E_{ch,i}}{E_{valley,i}}. \quad (13)$$

As seen from Eq. (13), the charging profiles has variable characteristics due to the time-varying function p_{valley} .

4. CASE STUDIES

The impact of the proposed coordinated charging algorithm on real microgrid data is quantified in this section.

4.1. Simulation Setup

4.1.1. Base Load and PV Generation Profile

In this study, a part of Cornell University microgrid is used. The sum of the daily average loading of Biotechnology building and Boyce Thompson Institute in the Cornell University Ithaca campus considered as the baseload profile [25]. The daily average of Geneva Solar PV data is used as PV generation profile [25]. Nominal capacity of the Geneva Solar PV Power plant, which consists of 6778 panels and has been operated since September 19, 2014, is 1776 kW. The data of loads and PV generation are recorded with a resolution of 15 minutes for one month.

The load and PV generation data were collected for the time from April 11th, 2016 to May 11th, 2016. Fig. 3 shows daily average load and PV generation profiles. The daily average, min, max, and standard deviation values of the load is 1034.4 kW, 836.6982 kW, 1193.9 kW and 138.0942, respectively. The daily average, min, and max values of the PV generation data is 601.85 kW, 0 kW, and 1757.1 kW, respectively. Since the load profile shows industrial load characteristics, its peak/lowest demand is not noticeable as it occurs in residential microgrids. The PV generation, however, has remarkable peak/lowest generation points, which are 0/1757.1 kW, as expected peak generation time is between 11am to 4 pm.

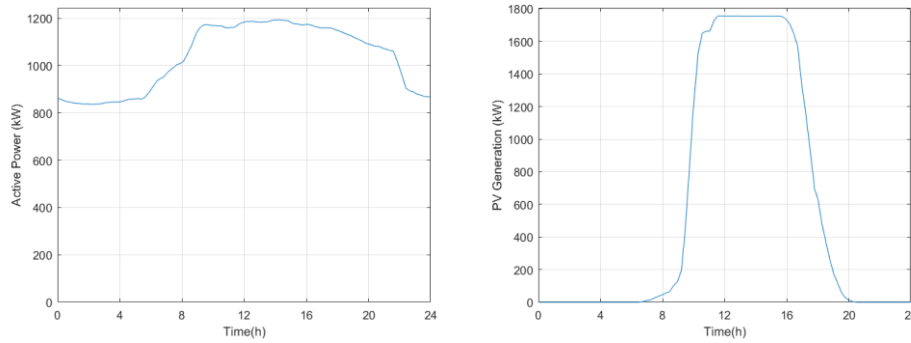


Figure 3. Daily average load and generation profiles of the microgrid

a) Base load, b) PV Generation.

4.1.2. PEV Specifications

Table 1 shows the specifications of PEV models used in this study. The number of PEVs is set to 200, which is corresponded to approximately 10% PEV penetration rate. The listed PEV models in Table 1 are distributed homogeneously among all vehicles. PEV mobility data is assumed to follow a Gaussian distribution. The mean and standard deviations are assumed to be (07:20, 2h), (16:30, 2.3h), and (50%, 10%) for plug-in and plug-off times, and SOC(%) level distributions, respectively [26]. The desired SOC(%) at the time of departure is set to 100% and vehicles are charged through their existing on-board chargers. It is assumed that only Mode-2 charging (single-phase, 32 A maximum) is employed for on-board charge using required EVSEs with the IEC 61851 standard cabling and conduit [27].

4.1.3. Algorithm Settings

The time horizon of 24 hours is discretized into time intervals of one minute. The simulation is run for 100 times to cover a considerable number of random PEV mobility trials and the mean of the simulations are reported as the result of the analysis.

Table 1. Types of PEVs and their specifications.

Vehicle make and model	Battery capacity (kWh)	PEV Range (km)	Max. 1- Φ charging power (kW)
BMW i3	18	110	7.4
Ford Focus	23	120	6.6
Nissan Leaf	24	150	6.6
Renault Zoe	22	100	7.4
Tesla Model S	85	350	10

4.2. Case studies

Three different case studies are carried out:

- i) *Uncoordinated charging*: This scenario is considered to demonstrate the impact of PEVs charging with uncoordinated charging strategy on the demand power profile. In this scenario, all PEVs start charging

at on-board charger power ratings immediately when they are connected to the microgrid at their arrival times.

- ii) *Shifted charging with uncontrolled strategy*: This scenario is to assess the impact of shifted charging with uncontrolled strategy. In this scenario, all PEVs are assumed to wait for charging till the PV generation is greater than or equal to the base load profile. Then, they start charging at on-board charger power ratings.
- iii) *Shifted charging with controlled strategy*: In this strategy, PEVs charging loads are shifted with a controlled manner to the time when the PV generation is considerable. The MGCC determines the time instants to start charging for each PEV according to its characteristics (battery and charger capacity, SOC level, and departure time) with Eq. (7).
- iv) *Coordinated charging*: This scenario is selected to investigate the impact of the proposed coordinated charging strategy. In this scenario, PEVs charging power references are dynamically adjusted by the MGCC to track the PV generation profile as explained in Section 3 with Eq. (8)-(13). Thus, PEVs are charged at variable power ratings.

The behavior of uncoordinated charging case on the microgrid and grid power profiles is shown in Fig. 4. Since most of the PEVs arrive before 10am, and their charging are performed at rated power in an uncoordinated fashion, the peak loading in the microgrid shows up before the PV generation reaches the rated value. Thus, the most of the peak loading is drawn from the grid, and the PV generation is not utilized efficiently. Fig. 5 shows the power profiles for the case of shifted charging with uncontrolled strategy. As observed from the figure, there is a salient undesired peak demand from the grid due to the charging all the PEVs simultaneously. However, the utilization of PV energy is increased since the initial time for charging process is shifted to the PV generation region. The behavior of shifted charging with controlled strategy on the microgrid and grid power profiles is shown in Fig. 6. With respect to uncontrolled shifted charging case, the utilization of PV generation within the microgrid is increased considerably. Moreover, the peak loading on the grid is reduced at the rate of ~30%. The performance of the proposed coordinated charging algorithm on the microgrid and grid power profiles are shown in Fig. 7. The proposed algorithm provides the PEV charging loads to track the PV generation profile successfully. Thus, the utilization of the PV energy is maximized, and the negative impact of PEV charging loads on the grid is minimized.

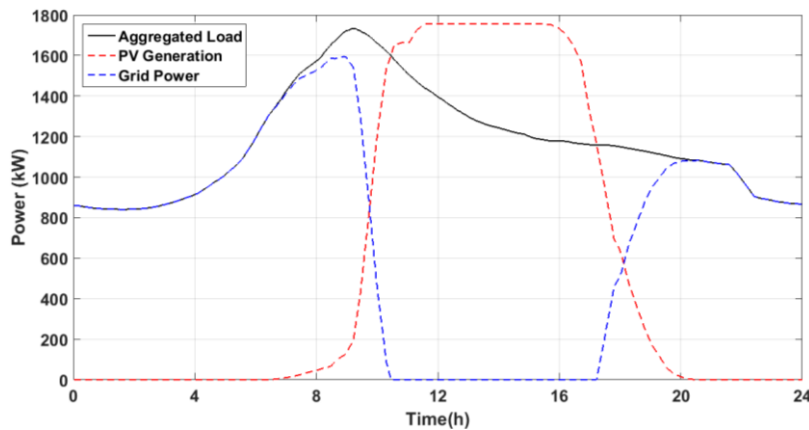


Figure 4. Power profiles for uncoordinated charging case.

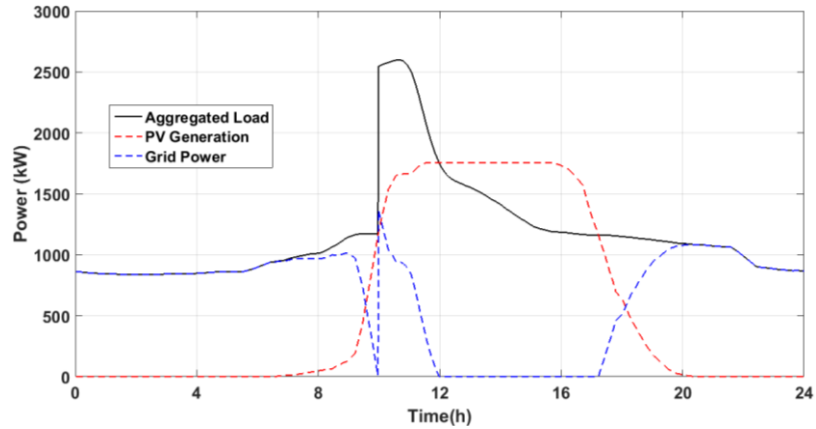


Figure 5. Power profiles for shifted charging with uncontrolled strategy case.

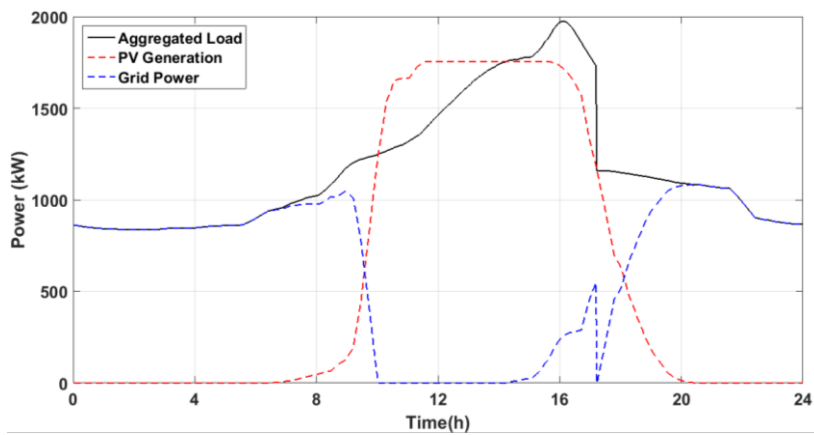


Figure 6. Power profiles for shifted charging with controlled strategy case.

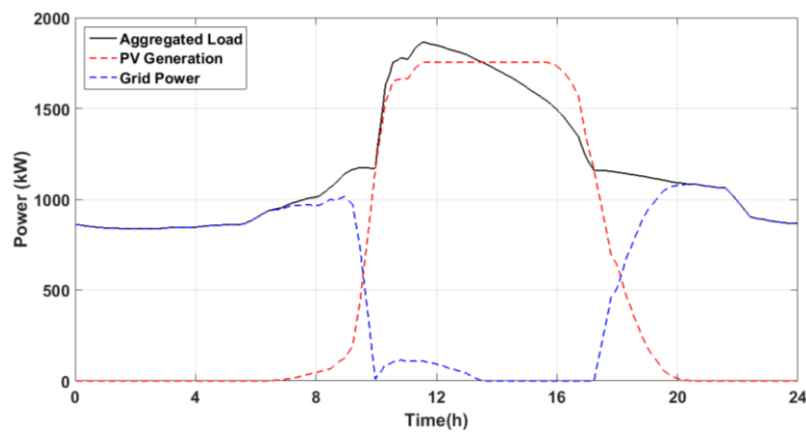


Figure 7. Power profiles for coordinated charging case.

The performance of the proposed coordinated charging algorithm is evaluated in terms of three parameters: (i) PV energy usage, (ii) energy supplied from the grid, (iii) peak demand power from the grid. PV energy usage (PVEU) refers to what extent the PV energy is used, and it is calculated as the ratio of daily used PV energy to daily total PV energy,

$$PVEU (\%) = \frac{\int (P_{aggr}(t) - P_{supply}(t)) dt}{\int P_{PV}(t) dt} \times 100 . \quad (14)$$

The energy (kWh) supplied from the grid is the daily total energy drawn from the main grid, which can be calculated by Eq.(13). Peak demand power from the grid (PDP) is the peak value of the power (kW) drawn from the main grid.

$$E_{demand} = \int ((P_{aggr}(t) - P_{solar}(t))) dt . \quad (15)$$

Table 2 summarizes the performance of the different charging strategies in terms of a fore mentioned metrics. Entries of the table represents the averages among 100 runs. Among the charging at rated power, controlled shifted charging gives better performance. In this case, with respect to the uncoordinated charging case, PVEU is increased by 16%, E_{demand} and PDP are decreased by almost 11% and 32% respectively. The best performance is obtained with the proposed coordinated charging algorithm. In the coordinated charging case, 96% of PV energy is utilized. Also, compared to the uncoordinated charging case, E_{demand} and PDP are decreased by approximately 3% and 32% respectively.

Table 2. Performance of different charging strategies.

Case Study	PVEU (%)	E_{demand} (kWh)	PDP (kW)
Uncoordinated charging	80	16962	1593
Uncontrolled Shifted charging	87	15972	1365
Controlled Shifted charging	93	15122	1082
Coordinated charging	96	14787	1082

5. CONCLUSIONS

The impact of PEV charging strategies in microgrid setting containing PV generation system has been investigated in this study. Two different coordinated charging strategies with constant (rated) and variable power rates have been proposed. The performance of proposed strategies has been quantified and compared with other charging methods using the real microgrid data. The obtained results demonstrate that the proposed charging strategy achieves increased utilization of PV generation efficiently, and reduced dependency on the power grid substantially. In addition, the charging strategy always ensures the desired SOC level at departure time in terms of PEV user perspective.

SYMBOLS

$C_{B,i}$: Nominal battery capacity (kWh)

$E_{ch,i}$: Energy (kWh) required to fully charge the i^{th} PEV

E_{demand} :Daily total energy(kWh)supplied by the main grid

$E_{valley,i}$: Energy of the valley (kWh) for the i^{th} PEV

n : Number of PEVs

$p_{ch,i}(t)$: Charging power (kW) for the i^{th} PEV at time t

$p_{base}(t)$: Microgrid base load (kW) at time t

$\hat{p}_{base}(t)$:Forecasted base load(kW) at time t

$p_{PV}(t)$: Power (kW) generated by the PV system at time t

$\hat{p}_{PV}(t)$: Forecasted PV output power (kW) at time t

$p_{\text{supply}}(t)$: Power (kW) supplied from the grid at time t

P_i^{rated} : Rated charging power (kW) of i^{th} PEV

p_{valley} : Valley power(kW)

$\text{SOC}_{\text{initial},i}$: SOC level of that PEV at arrival time

$T_{\text{ch},i}$: Total charging time (h) for the i^{th} PEV to be fully charged at rated charging power

T_i : Required charging time interval for i^{th} PEV at variable power profiles

t_1 : The first time of intersection between PV output and base load power profiles

t_2 : The second time of intersection between PV output and base load power profiles

$t_{\text{start},i}$: Initial time to start charging for i^{th} PEV

$t_{\text{finish},i}$: Charging stop times for i^{th} PEV

$t_{\text{arr},i}$: Arrival time (h) of the i^{th} PEV vehicle

$t_{\text{dept},i}$: Departure time (h) of the i^{th} PEV vehicle

η : Charger efficiency

α : Tracking factor

REFERENCES

- [1] Ahn C. and Peng H., “Decentralized and Real-Time Power Dispatch Control for an Islanded Microgrid Supported by Distributed Power Sources,” *Energies*, pp. 6439–6454, 2013.
- [2] Gholami A., Aminifar F., and Shahidehpour M., “Front Lines Against the Darkness,” *IEEE Electr. Mag.*, no. March, pp. 18–24, 2016.
- [3] Gouveia C., Moreira C. L., Lopes J. A. P., Varajao D., and Araujo R. E., “Microgrid service restoration: The role of plugged-in electric vehicles,” *IEEE Ind. Electron. Mag.*, vol. 7, no. 4, pp. 26–41, 2013.
- [4] Gouveia C., Moreira J., Moreira C. L., and Lopes J. A. P., “Coordinating storage and demand response for microgrid emergency operation,” *IEEE Trans. Smart Grid*, vol. 4, no. 4, pp. 1898–1908, 2013.
- [5] San Román T. G., Momber I., Abbad M. R., and Sánchez Miralles Á., “Regulatory framework and business models for charging plug-in electric vehicles: Infrastructure, agents, and commercial relationships,” *Energy Policy*, vol. 39, no. 10, pp. 6360–6375, 2011.
- [6] Sortomme E., Hindi M. M., MacPherson S. D. J., and Venkata S. S., “Coordinated charging of plug-in hybrid electric vehicles to minimize distribution system losses,” *IEEE Trans. Smart Grid*, vol. 2, no. 1, pp. 186–193, 2011.
- [7] García-Villalobos J., Zamora I., San Martín J. I., Asensio F. J., and Aperribay V., “Plug-in electric vehicles in electric distribution networks: A review of smart charging approaches,” *Renew. Sustain. Energy Rev.*, vol. 38, pp. 717–731, 2014.
- [8] Deilami S., Masoum A. S., Moses P. S., and Masoum M. A. S., “Real-time coordination of plug-in electric vehicle charging in smart grids to minimize power losses and improve voltage profile,” *IEEE Trans. Smart Grid*, vol. 2, no. 3, pp. 456–467, 2011.

- [9] Tan K. M., Ramachandaramurthy V. K., and Yong J. Y., “Integration of electric vehicles in smart grid: A review on vehicle to grid technologies and optimization techniques,” *Renew. Sustain. Energy Rev.*, vol. 53, pp. 720–732, 2016.
- [10] Kou P., Liang D., Gao L., and Gao F., “Stochastic coordination of plug-in electric vehicles and wind turbines in microgrid: a model predictive control approach,” *IEEE Trans. Smart Grid*, vol. 7, no. 3, pp. 1537-1151, 2016.
- [11] Wu T., Yang Q., Bao Z., and Yan W., “Coordinated energy dispatching in microgrid with wind power generation and plug-in electric vehicles,” *IEEE Trans. Smart Grid*, vol. 4, no. 3, pp. 1453–1463, 2013.
- [12] Abdelaziz M.M.A., Shaaban M.F., Farag H.E., and El-Saadany E.F., “A multistage centralized control scheme for islanded microgrids with PEVs,” *IEEE Trans. Sustain. Energy*, vol. 5, no. 3, pp. 927-937, 2014.
- [13] Kennel F., Gorges D., and Liu S., “Energy management for smart grids with electric vehicles based on hierarchical MPC ,” *IEEE Trans. Ind. Informatics*, vol. 9, no. 3, pp. 1528-1537, 2013.
- [14] Su W., Wang J., and Roh J., “Stochastic energy scheduling in microgrids with intermittent renewable energy resources,” *IEEE Trans. Smart Grid*, vol. 5, no. 4, pp. 1876–1883, 2014.
- [15] Carpinelli G., Mottola F., and Proto D., “ Optimal scheduling of a microgrid with demand response resources,” *IET Gen. Trans. & Dist.*, vol. 8, no. 12, pp. 1891-1899, 2014.
- [16] Liu N., Chen Q., Liu J., Lu X., Li P., Lei J., and Zhang J., “A Heuristic Operation Strategy for Commercial Building Microgrids Containing EVs and PV System,” *IEEE Trans. Ind. Electron.*, vol. 62, no. 4, pp. 2560–2570, 2015.
- [17] Wang G., Zhao J., Wen F., Xue Y., and Ledwich G., “Dispatch strategy of PHEVs to mitigate selected patterns of seasonally varying outputs from renewable generation,” *IEEE Trans. Smart Grid*, vol. 6, no. 2, pp. 627–639, 2015.
- [18] Derakhshandeh S. Y., Masoum A. S., Deilami S., Masoum M. A. S., and Hamedani Golshan M. E., “Coordination of generation scheduling with PEVs charging in industrial microgrids,” *IEEE Trans. Power Syst.*, vol. 28, no. 3, pp. 3451–3461, 2013.
- [19] Mohamed A., Salehi V., Ma T., and Mohammed O., “Real-time energy management algorithm for plug-in hybrid electric vehicle charging parks involving sustainable energy,” *IEEE Trans. Sustain. Energy*, vol. 5, no. 2, pp. 577–586, 2014.
- [20] Malhotra A., Erdogan N., Binetti G., Schizas I.D. and Davoudi A., “Impact of charging interruptions in coordinated electric vehicle charging ,” *IEEE Global Conference on Signal and Information Processing*, Greater Washington, D.C., USA, December 7–9, 2016
- [21] Yilmaz M., and Krein P.T., “Review of the impact of vehicle-to-grid technologies on distribution systems and utility interfaces,” *IEEE Trans. Smart Grid*, vol. 28, no. 12, pp. 5673-5689, 2013.
- [22] Kisacikoglu M.C., Erden F., Erdogan N., “ A Distributed Smart PEV Charging Algorithm Based on Forecasted Mobility Energy Demand,” *IEEE Global Conference on Signal and Information Processing*, Greater Washington, D.C., USA, December 7–9, 2016.
- [23] Hong T., Fan S., Probabilistic electric load forecasting: A tutorial review, *International Journal of Forecasting*, 32(3), 914–938, 2016.
- [24] Junior, J. G. D. S. F., Oozeki, T., Ohtake, H., Shimose, K. I., Takashima, T., and Ogimoto, K., Forecasting Regional Photovoltaic Power Generation-A Comparison of Strategies to Obtain One-Day-Ahead Data, *Energy Procedia*, 57, 1337-1345, 2014.

- [25] (May 09, 2016). Cornell University, Energy Management and Control System (EMCS) Website. [Online]. Available: <http://portal.emcs.cornell.edu>.
- [26] Ahn C., Li C.-T., and Peng H., “Optimal decentralized charging control algorithm for electrified vehicles connected to smart grid,” *Journal of Power Sources*, vol. 196, no. 23, pp. 10 369–10 379, 2011.
- [27] IEC Std. 61851, Electric vehicle conductive charging system, 2010.